

More than just a GPCR ligand: structure-based discovery of thioridazine derivatives as Pim-1 kinase inhibitors†‡

Cite this: *Med. Chem. Commun.*, 2014, 5, 507

Wei Li,^{ab} Xiaobo Wan,^b Fanqi Zeng,^b Yuting Xie,^b Yanli Wang,^b Wei Zhang,^b Li Li^b and Niu Huang^{*ba}

Pim-1 kinase is a serine/threonine kinase which plays an important role in cell proliferation and differentiation. The Pim-1 kinase expression is elevated in leukemia and prostate cancer. Accordingly, we employed a structure-based hierarchical virtual screening approach to identify potential unknown Pim-1 kinase activity for existing drugs. Among the LOPAC library of pharmacologically active compounds, one top-ranked drug molecule thioridazine, a well-known antipsychotic agent which exerted its biological function as a dopamine receptor antagonist, showed low micromolar activity in the Pim-1 enzymatic assay. We determined the co-crystal structure of thioridazine bound with Pim-1 kinase, and defined the key elements of the pharmacophore by analyzing the structure–activity relationship of thioridazine analogues. In addition, we also assessed our pharmacophore by successfully predicting the Pim-1 activity of the selective Akt inhibitor, 10-DEBC. Our discovery of the unknown Pim-1 inhibitory activity of thioridazine and 10-DEBC might provide novel insights into understanding their molecular mechanism of action, and inspire the computation-driven multiple-target drug discovery.

Received 23rd January 2014
Accepted 4th February 2014
DOI: 10.1039/c4md00030g
www.rsc.org/medchemcomm

The target binding profile of a drug molecule is essential for understanding its mechanism of action (MOA), as its off-target binding propensities may lead to better clinical efficacy in some circumstances, while causing side effects in other cases. Many marketed drugs existing today were discovered serendipitously, and the elucidation of their MOA has been usually retrospective. Notably, their therapeutic efficacies were often attributed to their multiple target actions. One example is clozapine, it is one of the most successful atypical antipsychotic drugs, it was discovered half a century ago, and its clinical efficacy was reported to be associated with its promiscuous binding to dozens of G protein-coupled receptors (GPCRs).¹ Many compounds even designated as single-target drugs are in fact not as specific as originally expected, and have been discovered to bind to other targets. For example, Gleevec was initially designed to inhibit the abnormal tyrosine kinase BCR-ABL. Subsequently, it was shown to target several other kinases,

including c-KIT and PDGFR kinases, which led to its expanded clinical applications in advanced or metastatic gastrointestinal stromal tumor (GIST).^{2,3}

Experimentally testing all drugs on all potential biomolecular targets is practically impossible; therefore, computationally predicting the novel polypharmacology of drug molecules has recently attracted great interest in the field of drug discovery.^{4–6} One notable method is the development of a statistics-based chemoinformatics approach, similarity ensemble approach (SEA), which has been applied in systematically relating the ligand chemical similarity to biological targets.^{7–9} Complementary to such ligand-based approaches, protein structure-based methods require the structures of known targets to predict protein–ligand binding complexes, and to estimate the binding affinities, like the inverse docking protocol INVDOCK.^{10,11}

GPCRs and kinases are two most important drug target families, and many of their ligands are promiscuous within their own protein families. However, the ligand cross-reactivity between kinase inhibitors and GPCR ligands has rarely been reported. Interestingly, a well-known kinase drug, sorafenib, was identified to bind to 5-hydroxytryptamine receptors (5-HTRs) by computationally screening the FDA approved drug molecules against the modelled structure of the 5-HT_{2A} receptor.¹² Therefore, we were wondering whether we could discover known GPCR ligands with unexpected kinase activities by virtually screening GPCR ligands against therapeutically relevant kinases.

^aGraduate Program in Peking Union Medical College and Chinese Academy of Medical Sciences, Beijing 100730, China

^bNational Institute of Biological Sciences, Beijing No. 7 Science Park Road, Zhongguancun Life Science Park, Changping, Beijing 102206, China. E-mail: huangniu@nibs.ac.cn; Fax: +86-10-80720813; Tel: +86-10-80720645

† The authors have declared no conflict of interest.

‡ Electronic supplementary information (ESI) available: Pim-1 and thioridazine, Pim-1 and 10-DEBC complex crystallization, data collection, and structure determination. Modelled complex structures of chlorprothixene analogues, thioridazine, propionylpromazine and amitriptyline. Structural similarity analysis. See DOI: 10.1039/c4md00030g

The proviral integration site in Moloney murine leukemia virus (Pim) kinases are a family of proto-oncogenic serine/threonine kinases regulating several signalling pathways that are fundamental to cancer development and progression.¹³ As the most studied member of Pim kinases, Pim-1 kinase is highly expressed in a wide range of haematopoietic malignancies and solid cancers, especially in leukemia and prostate cancer.^{13,14} Pim-1 kinase adopts a typical kinase fold consisting of N-terminal and C-terminal domains linked by a hinge region. However, the presence of residue P123 in the hinge region disrupts the canonical hydrogen bonding pattern with the adenine moiety of ATP or bound inhibitors due to the lack of the hydrogen bond donor.^{15,16} This unique hinge region architecture suggests that Pim-1 kinase inhibitors might be structurally distinguishable from many classical kinase inhibitors. Therefore, we further asked whether we could discover the unexpected Pim-1 kinase activity of GPCR ligands.

In our continuous endeavor to computationally find novel ligand cross-reactivity,^{12,17} we employed a structure-based hierarchical virtual screening strategy^{18,19} in combination with experimental evaluation to explore the unknown Pim-1 kinase activity of existing drugs and chemical probes with known biological activity (Fig. 1). Briefly, we docked 1280 LOPAC library compounds (Sigma-Aldrich Corp.) against the ATP binding site of Pim-1 kinase (PDB ID:2J2I²⁰) using the fast-compute docking program DOCK 3.5.54.²¹ The automated docking pipeline as described previously^{22,23} includes the sphere generation, scoring grid and docking calculations. All generated docking poses were subjected to the MM-GB/SA refinement and rescoring procedure.^{18,24} The energy minimizations were performed using the Protein Local Optimization Program (PLOP) with an all-atom molecular-mechanics (MM) force field and a generalized born surface area (GB/SA) implicit solvent model with variable internal dielectric constant.²⁵ The ligand binding energy was computed by subtracting the energies of the optimized free ligand in solution and the free protein in solution from the optimized ligand-protein complex's energy in solution, accounting for protein-ligand interaction energy, desolvation energies of ligand and protein, and ligand strain energy. Finally, we visually examined the top 1% ranked poses, and chose the compounds of interest for experimental testing.

Interestingly, two well-known GPCR ligands, thioridazine and chlorprothixene analogues, were identified in the top 1% of

docking hits (ESI, Fig. S1†). Therefore, we measured the enzymatic inhibition activities of these two compounds using Homogeneous Time Resolved Fluorescence (HTRF) kinase assay as described previously.¹⁷ Thioridazine inhibited Pim-1 kinase with an IC₅₀ value of 6.89 μM (Fig. 2a) while the chlorprothixene analogue showed no inhibitory activity. Since the commercially available thioridazine is a mixture of racemic enantiomers, we tested the purified forms of both enantiomers obtained from Dr Jørn B. Christensen.²⁶ The racemic mixture (–/+), the dextrorotatory form (+) and the levorotatory form (–) did not show difference in Pim-1 inhibition activity (Table 1 and ESI, Fig. S2†). We also tested two additional dopamine receptor antagonists, amitriptyline and propionylpromazine. Both compounds adopted similar docking poses to thioridazine (ESI, Fig. S1†); however, the rank of their MM-GB/SA energy scores were below the top 1%. None of the compounds showed activity.

Thioridazine represents a novel class of Pim-1 inhibitors. We submitted thioridazine to the SEA server (<http://sea.bkslab.org>), but none of the kinases were predicted to be thioridazine's potential target based on ligand structural similarity. We also performed pair-wise similarity comparison of thioridazine

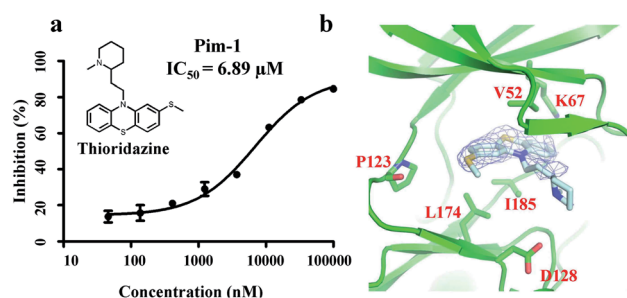


Fig. 2 (a) Dose–response inhibition of Pim-1 by thioridazine. The IC₅₀ value was determined from three independent tests. (b) Fitting dextrorotatory form (+) of thioridazine (gray) into an electron density map in the ATP binding-site of Pim-1. The sigma-A weighted 2Fo–Fc electron density map contoured at a level of 1.0σ. Coordinates and detailed methods for the solved crystal structure were deposited to the PDB with the accession ID 4IAA. Molecular images were generated with PyMOL.²⁷

Table 1 Inhibition of Pim-1 by thioridazine derivatives

Compound name	IC ₅₀ ^a (μM)
Thioridazine (–/+)	6.89 ± 1.51
Thioridazine (–)	7.39 ± 2.59
Thioridazine (+)	7.03 ± 2.52
NCI186055	8.16 ± 2.47
NCI186058	6.73 ± 0.45
NCI64076	34.0 ± 7.2% (100 μM)
b1	9.7 ± 2.1% (100 μM)
b2	22.6 ± 2.9% (100 μM)
b3	17.6 ± 8.7% (100 μM)
b4	8.70 ± 3.39
10-DEBC	1.28 ± 0.28

^a Data are shown as (mean values ± SD) from three independent determinations.

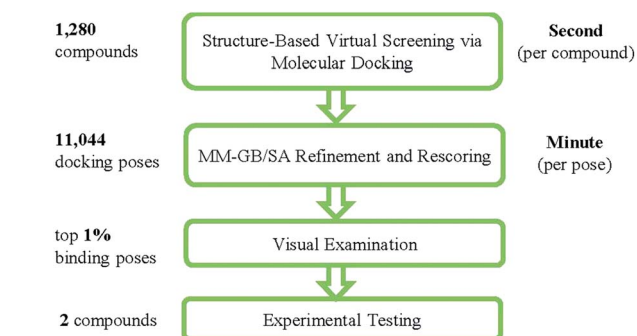


Fig. 1 Flowchart of our structure-based virtual screening strategy.

against the co-crystal inhibitors of Pim-1 using ChemMine Web Tools.²⁸ None of the calculated Tanimoto coefficients are greater than 0.35 (ESI, Table S1†). In addition, the structural similarity analysis against all reported 669 Pim-1 inhibitors in the ChEMBL database did not identify any structural analogues of thioridazine. Therefore, thioridazine could not be predicted as a Pim-1 inhibitor using these ligand-based approaches.

Next, we determined the X-ray crystal complex structure of Pim-1 kinase bound with thioridazine at 2.85 Å resolution (Fig. 2b). Note that we used the racemic mixture in the crystallization study due to the inadequate availability of pure enantiomers, and we fitted the dextrorotatory form (+) of thioridazine into the electron density map in the ATP-site. The detailed experimental procedure is included in the ESI (Table S2†). The overall structure of the Pim-1 kinase resembles published crystal structures. The crystal binding pose of thioridazine is consistent with our docking prediction with an RMSD value of 3 Å using the dextrorotatory form for comparison. The electron density of the phenothiazine group in thioridazine is very clear, it interacts favorably with hydrophobic residues V52, L174 and I185 in the ATP binding-site, while no hydrogen bond is formed between thioridazine and the kinase hinge region. Nevertheless, the weak electron density map features at the aliphatic chain and the piperidine ring of thioridazine suggest the conformational diversity and/or the ambiguous configurations of the piperidine ring in the racemic mixture.

To explore the key elements of the binding pharmacophore of thioridazine, we obtained three thioridazine analogues from the National Cancer Institute (NCI) compound library. Compounds NCI186055 and NCI186058, with a chloro or bromo group replacing the methylsulfanyl group on the phenothiazine ring of thioridazine, exhibited similar inhibitory activity to thioridazine (Fig. 3a and Table 1). This result was consistent with the crystallographic position of the methylsulfanyl group, which did not form direct contacts with binding-site residues by extending into the solvent (Fig. 2b). In contrast, compound NCI64076 was nearly inactive (Fig. 3a and Table 1). The major difference between NCI64076 and thioridazine was the length of the aliphatic chain bridging the piperidine ring and the phenothiazine scaffold, which may largely reduce the favorable electrostatic interaction between the positively charged nitrogen atom in the piperidine group and negatively charged residue D128. To further assess the contribution of the aliphatic amines, we synthesized and tested compound b4 along with three intermediates (Fig. 3b and Table 1). All three intermediate compounds were inactive while only compound b4 was as active as thioridazine, which could support the basic components of the pharmacophore: a tricyclic ring scaffold occupying the hydrophobic ATP binding-site, a bridging aliphatic chain with suitable length and an aliphatic amine group interacting with negatively charged residue D128.

Additionally, we noticed that one widely used selective Akt inhibitor, 10-DEBC²⁹ (Fig. 3c), satisfied our designated Pim-1 pharmacophore. As expected, 10-DEBC showed strong inhibitory activity with an IC₅₀ value of 1.28 μM. We also determined the X-ray crystal complex structure of 10-DEBC bound with Pim-1 (Fig. 4 and Table S2†). Comparing two co-crystal structures,

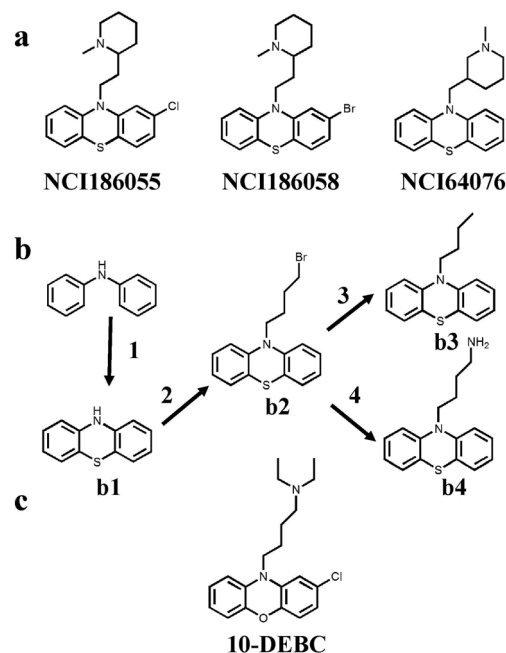


Fig. 3 (a) The chemical structures of the three thioridazine derivatives obtained from the National Cancer Institute. (b) Synthesis of phenothiazine derivatives. General synthetic approaches. Reagents: (1) sulfur, I₂, 170 °C, 2 h, 60%; (2) 1,4-dibromobutane, NaH, 25 °C, DMF, overnight, 78%; (3) NaN₃, DMSO-H₂O (5 : 1), 25 °C, 48 h, 55%; (4) H₂, Pd/C, MeOH, 50 °C overnight, 50%; (5) NaI, NH₃·H₂O, CsCO₃, DMF, 80 °C, 2 h, 80%. (c) Chemical structure of 10-DEBC.

the tricyclic scaffolds in both compounds overlap to a great extent while the methylsulfanyl group in thioridazine and the chloro group in 10-DEBC point in opposite directions. At the same crystallographic resolution of 2.85 Å, the electron density map in the 10-DEBC bound structure is sufficiently resolved to place the aliphatic chain and diethylamino group. The charged tertiary amine group in 10-DEBC forms a more favorable electrostatic interaction with residue D128 than thioridazine (3.5 Å in 10-DEBC vs. 4.5 Å in thioridazine), which may indicate the structural basis of strong inhibitory activity of 10-DEBC.

Thioridazine is an antipsychotic drug known to exert its biological function as a dopamine receptor antagonist. Interestingly, thioridazine has recently been found to selectively target the neoplastic cells, and impair human somatic cancer stem cells capable of *in vivo* leukemic disease initiation without showing effects on normal blood stem cells.³⁰ The authors proposed that dopamine receptors might serve as biomarkers involved in diverse malignancies. However, it is not clear whether thioridazine's Pim-1 kinase inhibition activity might also contribute to its effect of eradicating cancer stem cells. Several pieces of experimental evidence are available to support our hypothesis. Firstly, Pim-1 kinase has been shown to express in haematopoietic stem cells and embryonic stem cells.¹³ Pim-1 mediates the homing and migration of hematopoietic cells through phosphorylation of chemokine receptor 4 (CXCR4).³¹ Pim-1 kinase is also involved in mouse embryonic stem cell self-renewal.³² Secondly, Pim-1 plays an important physiological role in c-Myc driven tumorigenesis *via* effective oncogene

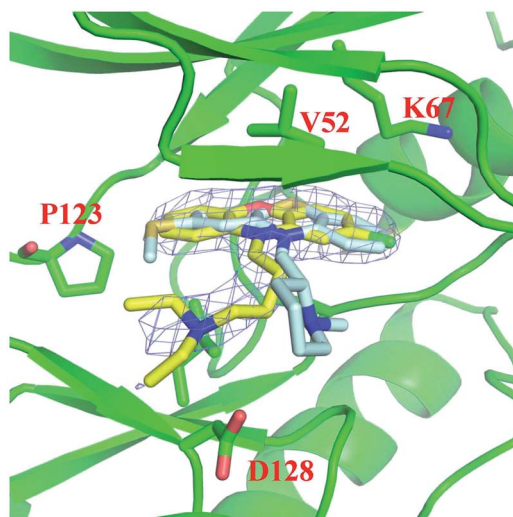


Fig. 4 The detailed view of the Pim-1 kinase domain with 10-DEBC (PDB code: 4MED) compared with thioridazine (PDB code: 4IAA). The protein is shown in a green cartoon representation. The compound 10-DEBC is represented as orange sticks and thioridazine as cyan sticks. Several important binding site residues are highlighted. The sigma-A weighted 2Fo-Fc electron density map contoured at a level of 1.0 σ .

collaboration, where the elevated expression level of Pim-1 is often observed in the context of increased c-Myc levels.¹³ Pim-1 phosphorylates c-Myc to stabilize c-Myc *in vivo* and to enhance the c-Myc transforming activity,³³ where c-Myc exerts a critical function in both self-renewal and differentiation of stem cells and early progenitor cells.³⁴ Thirdly, elevated levels of Pim-1 kinase have been observed in leukemia cancer cells.³⁵ Nevertheless, the mechanism of Pim-1 inhibition by thioridazine in cancer stem cell differentiation requires further elucidation.

In addition, thioridazine was reported to induce apoptosis in ovarian, cervical and endometrial cancer cells by targeting the Akt/mTOR signalling pathway, where the phosphorylation levels of Akt and 4E-BP1 were decreased by thioridazine treatment.^{36,37} Notably, both Akt and Pim-1 kinases share several common substrates that are involved in apoptosis.³⁸ Pim-1 inhibitor has recently been reported to reduce the phosphorylation of Akt.³⁹ 4E-BP1, one of the best characterized targets of the mTOR complex, was identified as a substrate of Pim-1 kinase.⁴⁰ Therefore, it is likely that thioridazine induces apoptosis by modulating the Akt/mTOR signalling pathway through Pim-1 inhibition.

In the present study, we also predicted the Pim-1 activity of a selective Akt inhibitor, 10-DEBC, based on our derived pharmacophore from thioridazine derivatives. Our biochemical and structural analysis validated its Pim-1 inhibitory activity. 10-DEBC was reported to be a micromolar inhibitor of Akt (5 μ M).²⁹ However, it was also reported to induce autophagy through an Akt-independent mechanism in neurons.⁴¹ Our results suggest that the cellular functions of 10-DEBC might be related to its Pim-1 inhibitory activity.

In summary, a selective dopamine receptor antagonist, thioridazine, was identified to be a low micromolar inhibitor of

Pim-1 kinase by a structure-based hierarchical virtual screening approach. The cocrystal structure, SAR study and pharmacophore evaluation indicated that a tricyclic scaffold with a suitable aliphatic side chain bridged tertiary amine might present a novel class of Pim-1 inhibitors. Moreover, a selective Akt inhibitor, 10-DEBC, possessing the key pharmacophore elements was shown to exhibit strong *in vitro* Pim-1 activity. Therefore, it is intriguing whether the Pim-1 inhibitory activity of thioridazine and 10-DEBC contributes to their mode of action. We hope that our present results will not only provide a novel scaffold for Pim-1 inhibitor design, but also inspire the computation-driven multiple-target drug discovery.

Acknowledgements

We thank the National Cancer Institute (NCI) for providing the compounds. We thank Dr Jørn B. Christensen (University of Copenhagen, Denmark) for generously providing us the pure enantiomers of thioridazine. We also thank Dr Andrew Christofferson for proofreading. Computational resource was supported by the Supercomputing Center of Chinese Academy of Sciences (SCCAS). Financial support from the Chinese Ministry of Science and Technology "973" Grant 2011CB812402 (to NH).

References

- 1 B. L. Roth, D. J. Sheffler and W. K. Kroeze, *Nat. Rev. Drug Discovery*, 2004, **3**, 353–359.
- 2 R. Capdeville, E. Buchdunger, J. Zimmermann and A. Matter, *Nat. Rev. Drug Discovery*, 2002, **1**, 493–502.
- 3 M. A. Fabian, W. H. Biggs, 3rd, D. K. Treiber, C. E. Atteridge, M. D. Azimioara, M. G. Benedetti, T. A. Carter, P. Ciceri, P. T. Edeen, M. Floyd, J. M. Ford, M. Galvin, J. L. Gerlach, R. M. Grotzfeld, S. Herrgard, D. E. Insko, M. A. Insko, A. G. Lai, J. M. Lelias, S. A. Mehta, Z. V. Milanov, A. M. Velasco, L. M. Wodicka, H. K. Patel, P. P. Zarrinkar and D. J. Lockhart, *Nat. Biotechnol.*, 2005, **23**, 329–336.
- 4 S. Peng, X. Lin, Z. Guo and N. Huang, *Curr. Top. Med. Chem.*, 2012, **12**, 1363–1375.
- 5 J. B. Brown and Y. Okuno, *Chem. Biol.*, 2012, **19**, 23–28.
- 6 A. L. Hopkins, *Nat. Chem. Biol.*, 2008, **4**, 682–690.
- 7 M. J. Keiser, B. L. Roth, B. N. Armbruster, P. Ernsberger, J. J. Irwin and B. K. Shoichet, *Nat. Biotechnol.*, 2007, **25**, 197–206.
- 8 M. J. Keiser, V. Setola, J. J. Irwin, C. Laggner, A. I. Abbas, S. J. Hufeisen, N. H. Jensen, M. B. Kuijer, R. C. Matos, T. B. Tran, R. Whaley, R. A. Glennon, J. Hert, K. L. Thomas, D. D. Edwards, B. K. Shoichet and B. L. Roth, *Nature*, 2009, **462**, 175–181.
- 9 E. Lounkine, M. J. Keiser, S. Whitebread, D. Mikhailov, J. Hamon, J. L. Jenkins, P. Lavan, E. Weber, A. K. Doak, S. Cote, B. K. Shoichet and L. Urban, *Nature*, 2012, **486**, 361–367.
- 10 Y. Z. Chen and C. Y. Ung, *J. Mol. Graph. Modell.*, 2001, **20**, 199–218.
- 11 Y. Z. Chen and D. G. Zhi, *Proteins*, 2001, **43**, 217–226.

- 12 X. Lin, X. P. Huang, G. Chen, R. Whaley, S. Peng, Y. Wang, G. Zhang, S. X. Wang, S. Wang, B. L. Roth and N. Huang, *J. Med. Chem.*, 2012, **55**, 5749–5759.
- 13 M. C. Nawijn, A. Alendar and A. Berns, *Nat. Rev. Cancer*, 2011, **11**, 23–34.
- 14 N. Ogawa, H. Yuki and A. Tanaka, *Expert Opin. Drug Discovery*, 2012, **7**, 1177–1192.
- 15 A. Kumar, V. Mandiyan, Y. Suzuki, C. Zhang, J. Rice, J. Tsai, D. R. Artis, P. Ibrahim and R. Bremer, *J. Mol. Biol.*, 2005, **348**, 183–193.
- 16 S. Schenone, C. Tintori and M. Botta, *Curr. Pharm. Des.*, 2010, **16**, 3964–3978.
- 17 X. Wan, W. Zhang, L. Li, Y. Xie, W. Li and N. Huang, *J. Med. Chem.*, 2013, **56**, 2619–2629.
- 18 N. Huang, C. Kalyanaraman, J. J. Irwin and M. P. Jacobson, *J. Chem. Inf. Model.*, 2006, **46**, 243–253.
- 19 R. Cao, M. Liu, M. Yin, Q. Liu, Y. Wang and N. Huang, *J. Chem. Inf. Model.*, 2012, **52**, 2730–2740.
- 20 O. Fedorov, B. Marsden, V. Pogacic, P. Rellos, S. Muller, A. N. Bullock, J. Schwaller, M. Sundstrom and S. Knapp, *Proc. Natl. Acad. Sci. U. S. A.*, 2007, **104**, 20523–20528.
- 21 D. M. Lorber and B. K. Shoichet, *Curr. Top. Med. Chem.*, 2005, **5**, 739–749.
- 22 N. Huang, B. K. Shoichet and J. J. Irwin, *J. Med. Chem.*, 2006, **49**, 6789–6801.
- 23 J. J. Irwin, B. K. Shoichet, M. M. Mysinger, N. Huang, F. Colizzi, P. Wassam and Y. Cao, *J. Med. Chem.*, 2009, **52**, 5712–5720.
- 24 N. Huang, C. Kalyanaraman, K. Bernacki and M. P. Jacobson, *Phys. Chem. Chem. Phys.*, 2006, **8**, 5166–5177.
- 25 K. Zhu, M. R. Shirts and R. A. Friesner, *J. Chem. Theory Comput.*, 2007, **3**, 2108–2119.
- 26 J. B. Christensen, O. Hendricks, S. Chaki, S. Mukherjee, A. Das, T. K. Pal, S. G. Dastidar and J. E. Kristiansen, *PLoS One*, 2013, **8**, e57493.
- 27 W. L. DeLano, *The PyMOL Molecular Graphics System*, DeLano Scientific, San Carlos, CA, USA, 2002, computer program.
- 28 T. W. Backman, Y. Cao and T. Girke, *Nucleic Acids Res.*, 2011, **39**, W486–W491.
- 29 K. N. Thimmaiah, J. B. Easton, G. S. Germain, C. L. Morton, S. Kamath, J. K. Buolamwini and P. J. Houghton, *J. Biol. Chem.*, 2005, **280**, 31924–31935.
- 30 E. Sachlos, R. M. Risueno, S. Laronde, Z. Shapovalova, J. H. Lee, J. Russell, M. Malig, J. D. McNicol, A. Fiebig-Comyn, M. Graham, M. Levadoux-Martin, J. B. Lee, A. O. Giacomelli, J. A. Hassell, D. Fischer-Russell, M. R. Trus, R. Foley, B. Leber, A. Xenocostas, E. D. Brown, T. J. Collins and M. Bhatia, *Cell*, 2012, **149**, 1284–1297.
- 31 R. Grundler, L. Brault, C. Gasser, A. N. Bullock, T. Dechow, S. Woetzel, V. Pogacic, A. Villa, S. Ehret, G. Berridge, A. Spoo, C. Dierks, A. Biondi, S. Knapp, J. Duyster and J. Schwaller, *J. Exp. Med.*, 2009, **206**, 1957–1970.
- 32 I. Aksoy, C. Sakabedoyan, P. Y. Bourillot, A. B. Malashicheva, J. Mancip, K. Knoblauch, M. Afanassieff and P. Savatier, *Stem Cells*, 2007, **25**, 2996–3004.
- 33 Y. Zhang, Z. Wang, X. Li and N. S. Magnuson, *Oncogene*, 2008, **27**, 4809–4819.
- 34 M. J. Murphy, A. Wilson and A. Trumpp, *Trends Cell Biol.*, 2005, **15**, 128–137.
- 35 R. Amson, F. Sigaux, S. Przedborski, G. Flandrin, D. Givol and A. Telerman, *Proc. Natl. Acad. Sci. U. S. A.*, 1989, **86**, 8857–8861.
- 36 S. Kang, S. M. Dong, B. R. Kim, M. S. Park, B. Trink, H. J. Byun and S. B. Rho, *Apoptosis*, 2012, **17**, 989–997.
- 37 S. B. Rho, B. R. Kim and S. Kang, *Gynecol. Oncol.*, 2011, **120**, 121–127.
- 38 M. A. Sussman, *Expert Rev. Cardiovasc. Ther.*, 2009, **7**, 929–938.
- 39 A. T. Fathi, O. Arowojolu, I. Swinnen, T. Sato, T. Rajkhowa, D. Small, F. Marmsater, J. E. Robinson, S. D. Gross, M. Martinson, S. Allen, N. C. Kallan and M. Levis, *Leuk. Res.*, 2012, **36**, 224–231.
- 40 W. W. Chen, D. C. Chan, C. Donald, M. B. Lilly and A. S. Kraft, *Mol. Cancer Res.*, 2005, **3**, 443–451.
- 41 A. S. Tsvetkov, J. Miller, M. Arrasate, J. S. Wong, M. A. Pleiss and S. Finkbeiner, *Proc. Natl. Acad. Sci. U. S. A.*, 2010, **107**, 16982–16987.